Food Chemistry 382 (2022) 132319

Contents lists available at ScienceDirect

Food Chemistry

journal homepage: www.elsevier.com/locate/foodchem

The formation of starch-lipid complexes by microwave heating

Xuemin Kang [a,b,c], Siqiang Jia [a,c], Wei Gao [a,b,c], Bin Wang [a,b,c], Xiaolei Zhang [b], Yaoqi Tian [d], Qingjie Sun [e], Mohammed Atef [f], Bo Cui [a,b,c,*], A.M. Abd El-Aty [b,f,g,*]

[a] State Key Laboratory of Biobased Material and Green Papermaking, Qilu University of Technology, Shandong Academy of Sciences, Jinan 250353, China
[b] Department of Food Science and Engineering, Shandong Agricultural University, Taian 271018, China
[c] School of Food Science and Engineering, Qilu University of Technology, Shandong Academy of Sciences, Jinan, Shandong 250353, China
[d] The State Key Laboratory of Food Science and Technology, Jiangnan University, Wuxi 214122, 6 China
[e] College of Food Science and Engineering, Qingdao Agricultural University, Qingdao 266109, Shandong, China
[f] Department of Pharmacology, Faculty of Veterinary Medicine, Cairo University, 12211 Giza, Egypt
[g] Department of Medical Pharmacology, Medical Faculty, Ataturk University, Erzurum, Turkey

ARTICLE INFO

Keywords:
Wheat starch
Starch-lipid complexes
Water bath heat treatment
Microwave heat treatment
Diffraction pattern
Starch digestibility

ABSTRACT

This study investigated the impact of microwave treatment on the formation of starch-lipid complexes, and physicochemical properties of wheat starch (WS) fortified with lipids, such as lauric acid (LA), glycerol monolaurate (GML), and stearic acid (SA). Specimens were prepared using a conventional water bath and microwave heating and evaluated using macrostructural and microstructural analyses. Iodine staining and scanning electron microscopy revealed interplay between WS and LA. Diffraction peaks around 7.5°, 13°, and 20° and the absence of the absorption band in the 2850 cm^{-1} were observed in microwave treated WS-lipid samples than conventional water bath samples. Further, more type I complexes were formed in WS-LA microwave-assisted samples, as demonstrated by differential scanning calorimetry. Additionally, more resistant starch was formed in specimens treated by microwave than water bath treated counterparts, the finding that was proved by *in vitro* enzymatic hydrolysis. In short, the current study may suggest the applications of microwave treatment in foods for hypoglycemia.

1. Introduction

Amylose, the essentially linear glucose polymer of starch, is a well-known host molecule that forms higher-order inclusion complexes with suitable guest molecules, such as iodine, alcohols, lipids, and hydrophobic organic polymers (Kadokawa, Kaneko, Nagase, Takahashi & Tagaya, 2015; Nimz, Gessler, Isabel, Sheldrick & Saenger, 2004; Rodriguez-Garcia et al., 2021). The amylose left-handed single helical inclusion complexes are often called amylose–lipid complexes. The complexes between starch and lipids, which readily occur when starch is subjected to heat (known as the resistant starch type 5 (RS_5)), appear to decrease the susceptibility of the starch granules to enzymatic digestion (Buddrick, Jones, Hughes, Kong & Small, 2015).

Targeting weight and managing type II diabetes have spurred remarkable growth in methodologies used to supplement the resistant starch (RS) content in starchy foods. In particular, the RS_5 that can carry essential fatty acids into the small intestine has attracted a great deal of attention (Putseys, Lamberts & Delcour, 2010; Siegfried, 2007). The approaches for the production of amylose–lipid complexes include the classical synthesis method, in which starch and lipids were added into a solvent (water, dimethyl sulfoxide, acid or alkali solutions) and treated at 90-100℃ (Biliaderis, Page, Slade & Sirett, 1985; Eliasson & Krog, 1985; Gelders, Vanderstukken, Goesaert & Delcour, 2004; Karkalas, Ma, Morrison & Pethrick, 1995; Le-Bail et al., 2015; Zhou, Robard, Helliwell & Blanchard, 2007). Alternatively, the complexes can be formed through the enzymatic method, in which short-chain amylose is synthesized by phosphorylase and then interact with lipids (Gelders, Goesaert, Delcour, 2005; Putseys, Derde, Lamberts, Goesaert & Delcour, 2009). Previous studies have stated that the formation and physicochemical characteristics of starch-lipid inclusion complexes could be linked to amylose content, pH of the solution, temperature, the carbon atom number, and degree of saturation of fatty acids (Karkalas, Ma, Morrison & Pethrick, 1995; Kang et al., 2021; Putseys, Derde, Lamberts, Goesaert & Delcour, 2009; Soong, Goh & Henry, 2013). Additionally,

* Corresponding authors: Qilu University of Technology (Shandong Academy of Sciences), Daxue Road, Changqing District, Jinan, Shandong Province 250353, China.
E-mail address: abdelaty44@hotmail.com (A.M. Abd El-Aty).

https://doi.org/10.1016/j.foodchem.2022.132319
Received 6 March 2021; Received in revised form 7 January 2022; Accepted 30 January 2022
Available online 4 February 2022

multiple studies have recently paid much attention to preparation methods that could advance the formation of inclusion complexes, such as physical (Le-Bail et al., 2015; Sullivan, Hughes, Cockman & Small, 2018; Zheng et al., 2018), chemical (Galloway, Biliaderis & Stanley, 1989; Garcia, Pereira-Da-Silva, Taboga & Franco, 2016), and enzymatic methods (Cheng, Luo, Li & Fu, 2015; Liu, Gao, Zhang, Wu & Cui, 2020; Liu, Fang, Zhang, Zou & Cui, 2020). Of note, physical modification has recently become the most popular way to optimize food quality and safety against the backdrop of an eco-friendly society.

At variance to conventional heating (heat-moisture and annealing), microwave heating changes the proper orientation of dipoles (Yuan et al., 2020). Microwave radiation's electric and magnetic field vibrating around 5.0×10^9 times/s can lead to polar molecules' friction, collision, vibration, and a rapid increase in temperature (Ozel, Dag, Kilercioglu, Sumnu & Oztop, 2017; Yuan et al., 2020). Over the past few decades, several studies have reported changes in the physicochemical properties of starches after microwave treatment. For instance, NMR relaxometry was used to demonstrate the effect of microwave heating (at 800 W for 5–30 s) on starch–water interactions and gelatinization behaviour (Ozel et al., 2017). Further, dynamic measurement of starch granule swelling during microwave heating was described by Casasnovas & Anantheswaran (2016). Moreover, Fan et al. (2013a,b, & Fan et al., 2014) investigated the differences between microwave and conventional heating by NMR through relaxation times (T_1 and T_2), glass transition temperatures, small-angle X-ray scattering, thermogravimetry (TGA), and differential scanning calorimetry (DSC) operating at a power ranging from 1200 to 300 W at different time. They found similar trends between microwave and conventional heating and implied that fast microwave heating is more convenient in saving time and resources (Fan et al., 2013a; Fan et al., 2013b; Fan et al., 2013c; Fan et al., 2014). However, up to the author's knowledge, far too little attention has been paid to the effects of microwave heating on the formation of amylose–lipid crystalline structure. We hypothesized that starch could form an inclusion complex with lipids under suitable microwave heating. Herein, we characterized the amylose–lipid complexes formed in a high-moisture model system based on microwave heating and compared it with conventional water bath heating. We aimed to apply an efficient method for the formation of starch-guest inclusion complexes.

2. Materials and methods

2.1. Materials

Native wheat starch (WS), extracted from wheat flour (Wudeli Flour Group Co., Ltd, Hebei, China) with 87% carbohydrate, was procured from Baby Suqian Biotechnology Co., Ltd. (Jiangsu, China). Guest molecules, including LA (lauric acid), SA (stearic acid), and GML (glycerol monolaurate) with 98% purity, were all acquired from Tianjin Fuyu Chemical (Tianjin, China). α-amylase of 100 U/mg (CAS # 9032–08-0) and amyloglucosidase of 10×10^4 U/mL (CAS # 9032–08-0) were supplied by Sigma-Aldrich (St. Louis, MO, USA) and Yuanye Biotechnology (Shanghai, China), respectively. All other chemicals were of analytical grade unless otherwise specified.

2.2. Preparation of WS-lipid complex by conventional water bath and microwave heating

2.2.1. Preparation of WS-lipid complexes by conventional water bath heating

WS paste solution: WS (10 g) and 150 mL deionized water were mixed in a glass bottle with a breathable cap (diameter = 6 cm) and heated in a water bath to 100 ℃ with continuous stirring for one hour. Subsequently, fatty acids, LA, SA, and GML (0.3 g of each) were dispersed in 20 g absolute ethanol (≥99.7%) and respectively mixed with WS paste solution. The paste solution was maintained at 100 ℃ for another hour under continuous stirring. After cooling to 20 °C, the mixture was washed four times with absolute ethanol and centrifuged (TDL-5-A, Shanghai Anting Scientific Instrument Co., Ltd., Shanghai, China) at 5000 rpm for 15 min each time. Ultimately, the supernatant was discarded, and the residue was dried in an oven (Shanghai Boxun industrial Medical Instrument Factory, Shanghai, China) at 40 °C for 36 h. The dried samples are then ground into a fine powder and pass through a 60 mesh sieve (Heding Wire Mesh Co., Ltd, Hebei, China). Starch paste without lipid was used as a control.

2.3. Preparation of WS-lipid complexes by microwave heating

WS paste solution: WS (10 g) and 150 mL deionized water were mixed in a glass bottle without a cap (the height of the liquid column is 4.5 cm) and heated with an M3-L236E Midea microwave oven (Foshan, Guangdong, China) operating at a power of 900 W for 2 min. During microwave heat treatment, the temperature of samples increased from room temperature to 80 °C in the first min and 95 °C in the next 30 s; then, the heat treatment was suspended for 20 s followed by 30 s heating at the centre of the oven. After that, fatty acids, LA, SA, and GML (0.3 g of each) were dispersed in 20 g absolute ethanol and respectively added to the WS paste solution. Next, the mixture was heated in the microwave for another two min, with an interval of 20 s for 30 s heating. Other operations were the same as stated above. The temperature throughout the samples was measured during microwave heat treatment.

2.4. Microstructure and iodine staining analysis (ISA)

The Olympus BX53-P polarizing microscope (Tokyo, Japan) was used to characterize the microstructure, and iodine staining analysis of water bath and microwave treated WS-lipid complexes at a magnification of 400 × . Accurately weighed potassium iodide (3.6 g) and iodine (1.3 g) were dispersed in 10 mL deionized water, and then the volume was adjusted to 100 mL. The iodine solution should be diluted 300 times before staining.

2.5. Scanning electron microscope (SEM)

SEM (Hitachi Regulus 8220, Tokyo, Japan) operated at 15 kV was employed to image complex samples with a magnification of 5000 × . The samples were fixed with double-sided sticky carbon tape, coated with Au/ Pd.

2.6. Fourier transform infrared spectroscopy analysis (FTIR)

A NICOLET iS10 Thermo Fisher Scientific (Waltham, MA, USA) acquired the spectra of all water bath, and microwave treated WS-lipid complexes. A 70 mg KBr was mixed with 0.7 mg starch samples, and then a thin sheet with a diameter of 1.15 cm and a thickness of 0.2 mm was obtained by pressing at a pressure of 10 MPa for 30 s. The FTIR spectra were recorded between 4000 cm^{-1} to 400 cm^{-1}, and the absorbance ratio at 1047/1022 cm^{-1} was calculated after deconvolution.

The following formula calculated the absorption coefficient for each IR band:

$$A = \varepsilon cd$$

where A is absorbance, ε is molar absorption (extinction) coefficient, c is the concentration of a measured substance, and d is the sample thickness.

2.7. X-ray diffraction (XRD)

The water bath and microwave treated samples' diffraction patterns were measured using a Bruker-AXS X-ray diffraction analysis (Karlsruhe, Germany) executed at 40 kV, 40 mA, 2θ scanning from 5° to 40°. The

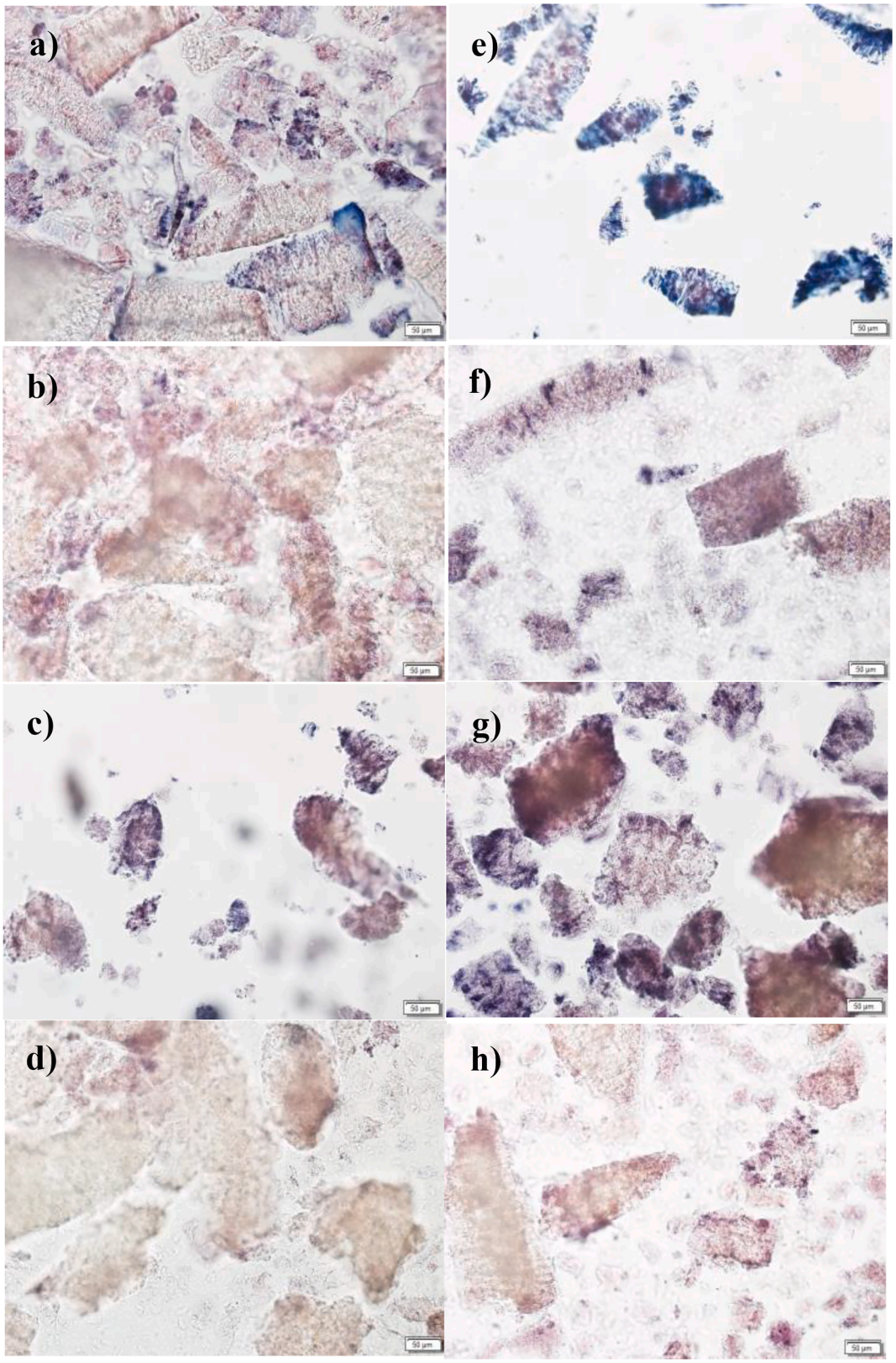

Fig. 1. Microscopically observed WS samples treated by microwave and water bath heating with and without lipid incorporation. (a-d): for microwave treatment, (e-h): for water bath treatment, (a & e) WS, (b & f) WS-LA, (c & g) WS-SA, (d & h) WS-GML.

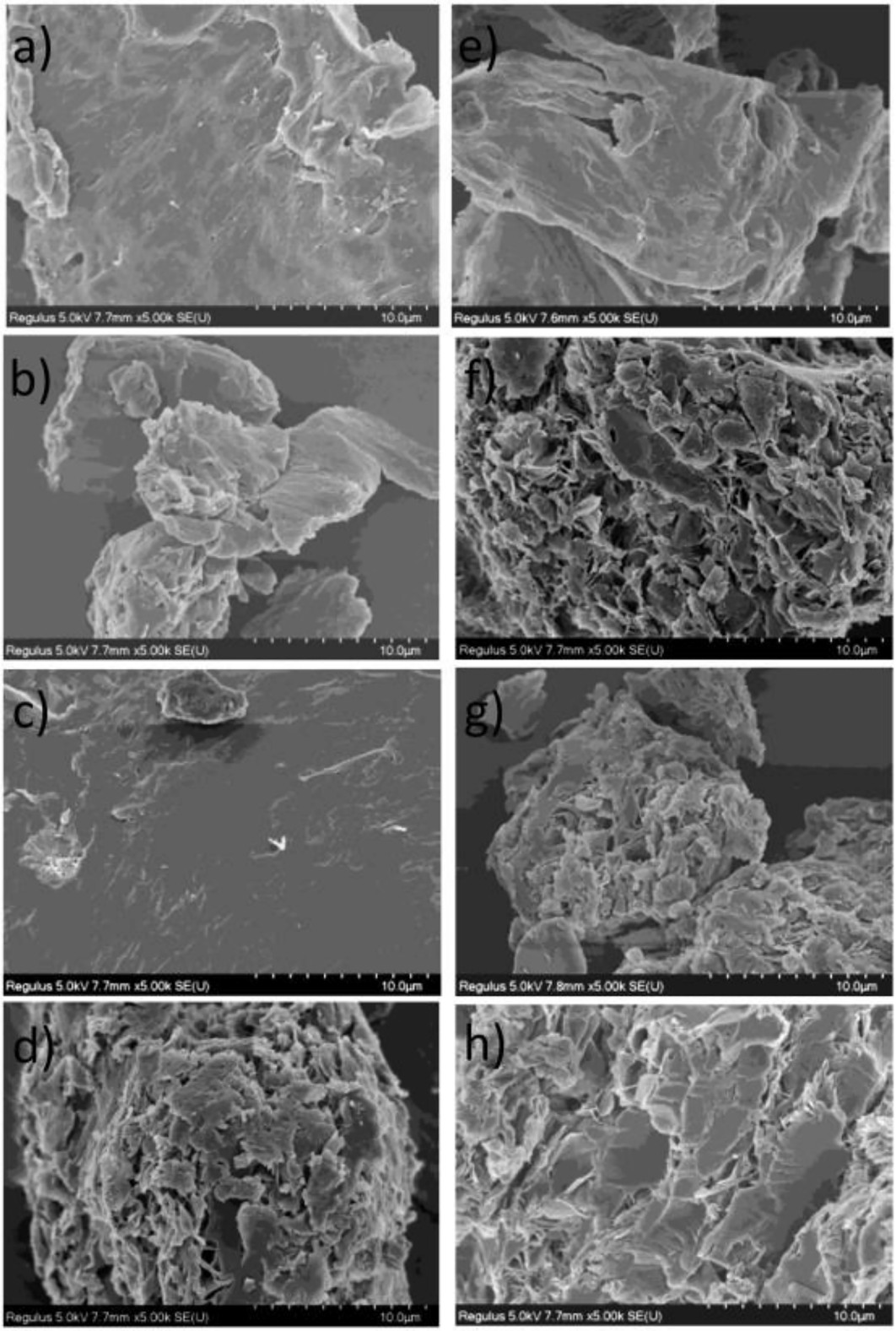

Fig. 2. Scanning electron microscope (SEM) images of microwave and water bath treated WS samples with and without lipid. (a-d): for microwave treatment, (e-h): for water bath treatment, (a & e) WS, (b & f) WS-LA, (c & g) WS-SA, (d & h) WS-GML.

JADE6 (America, TILAB) software calculated the relative crystallinity (RC).

$$RC = \frac{Crystal\ area}{Amorphous\ area + Crystal\ area}$$

2.8. Thermogravimetric analysis (TGA)

The thermal stability curves of water bath and microwave treated WS-lipid complexes were determined using a PerkinElmer thermal

analysis (STA-6000, Melbourne, Australia). Each sample (5 mg) was placed in an unsealed ceramic pan and heated from 30 ℃ to 700 ℃ at a rate of 20 ℃ per min. The second derivative was used to define the position of the proposed peaks.

2.9. Differential scanning calorimetry (DSC)

The DSC melting curves of the water bath and microwave treated WS-lipid complexes were determined by a NETZSCH DSC analyzer (DSC-200FC, NETZSCH, Selb, Germany). The powder sample (3 mg) was blended with 10 μL distilled water in an aluminum pan. Next, the sealed pans were placed at 20 ℃ for 24 h. The samples were heated from 40 to 140 °C at a heating rate of 10 °C per min.

2.10. In vitro digestibility

In vitro hydrolysis of all samples prepared by water bath and microwave heating was determined by Englyst & Cummings (1985) method with minor modifications. The dried powder (40 mg) was dispersed in acetate buffer (35 mL, pH 5.2). After that, 290 U/mL α-amylase and 30 U/mL amyloglucosidase enzyme mixture solution (acetate buffer, pH 5.2) 10 mL was added. Subsequently, the suspension was placed at a 37 °C water bath with continuous stirring at 150 rpm. The amount of glucose released during hydrolysis at 20, 60, 120, 180, and 240 min was determined using an SBA-40D glucose analyzer (Shandong Academy of Sciences, Jinan, China).

2.11. High-performance size-exclusion chromatography (HPSEC)

HPSEC method was carried out as provided by SANSHU Biotechnology Co., Ltd (Lin et al., 2016). Starch sample (5 mg) was thoroughly mixed with 5 mL DMSO (cellulose nanowhiskers) solution containing lithium bromide (0.5% *w/w*, Sigma) (DMSO/LiBr); heated at 80 °C for 3 h with a thermomixer. Various fractions' homogeneity and molecular weight were measured by size-exclusion chromatography with multi-angle light scattering (*SEC*-MALLS) paired with refractive index (RI) detection. The weight-and number-average molecular weight (Mw and Mn) and polydispersity index (Mw/Mn) of various fractions in DMSO/LiBr (0.5%, *w/w*) solution were measured on a DAWN® HELEOS^{TM}-II laser photometer (He-Ne laser, λ = 663.7 nm, Wyatt Technology Co., Santa Barbara, CA, USA) equipped with three tandem columns (300 × 8 mm, Shodex OHpak SB-805, 804, and 803; Showa Denko K.K., Tokyo, Japan); held at 60℃ using a model column heater. The flow rate was 0.3 mL/min. A differential refractive index detector (Optilab *T*-rEX, Wyatt Technology Co., Santa Barbara, CA, USA) was simultaneously connected to give the concentration of fractions and the dn/dc value. The dn/dc value of the fractions in the DMSO solution was determined to be 0.07 mL/g. Data were acquired and processed using ASTRA6.1 (Wyatt Technology).

2.12. Statistical analyses

The data are displayed as mean ± standard deviations (SDs). Significant differences between mean values were performed through the software Statistix 9. A P value < 0.05 was assigned as statistically significant.

3. Results and discussion

Herein, we have tested whether WS-lipid complexes could be formed and whether the structures and properties of the complexes would be consistent with those of the conventional hydrothermal (water bath) method after microwave treatment. First, the microstructure and iodine staining performance of WS-lipid complexes of all samples were compared. After that, the diffraction pattern, FTIR, and thermodynamics properties of microwave-treated WS-lipid complexes were compared with specimens prepared by a water bath. Then, the *in vitro* digestibility was investigated to gain insight into the digestion pattern of microwave-treated WS-lipid samples. Ultimately, the molecular weight size was determined by HPSEC through a multi-angle laser light scattering and differential detector.

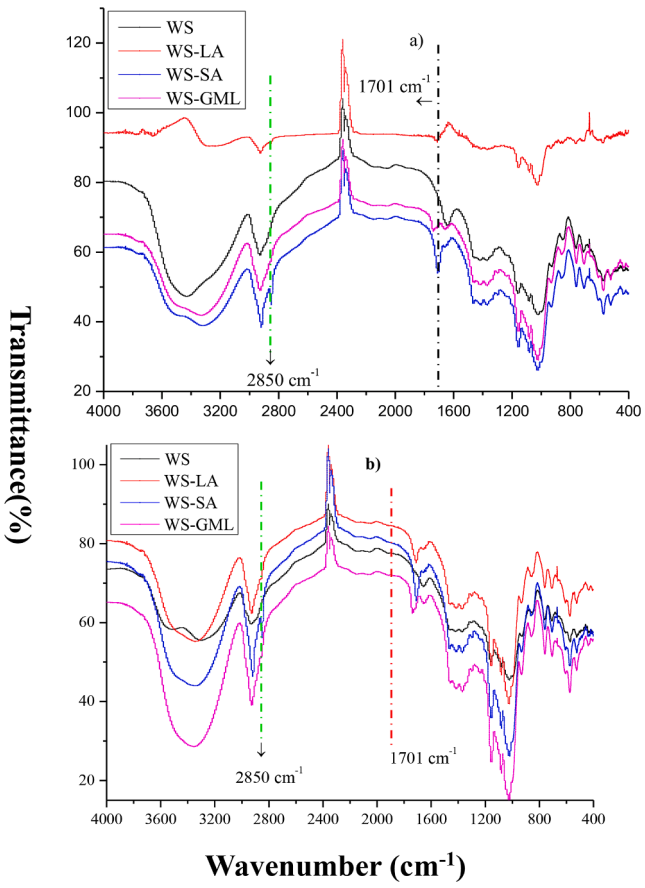

Fig. 3. Fourier transformation infrared spectroscopy (FTIR) of WS, WS-LA, WS-SA, and WS-GML samples. (a) water bath treatment, and (b) microwave treatment.

3.1. Microstructure and iodine staining analysis

The microscopic images of the iodine-stained WS-lipid complexes prepared by microwave and conventional water bath at a magnification level of 400 × are presented in Fig. 1 a-h. As shown in Fig. 1a, WS samples treated with microwave heating (without lipid incorporation) displayed a massive structure. A greater part was decorated purple and a few coloured blues by iodine solution. A small size structure with dark blue-purple colour was noticed for WS samples treated with conventional heating (without lipid incorporation). It is well-known that amylose gives a blue colour, whereas amylopectin gives a purple colour when stained with iodine (Evans, Mcnish & Thompson, 2003). The existence of the WS-lipid complex owes to the combination of amylose and lipids; in turn, the content of free amylose was decreased in samples incorporated with lipids. Hence, the blue colour was not noticed in Fig. 1 (b-d & f-h). Further, part of the block structure exhibited the colour of iodine solution, as shown in Fig. 1 (b & d). This result could be explained on the basis that the compact and ordered structure of WS-LA and WS-GML prepared by microwave (Fig. 1 b & d) cannot be stained with iodine solution.

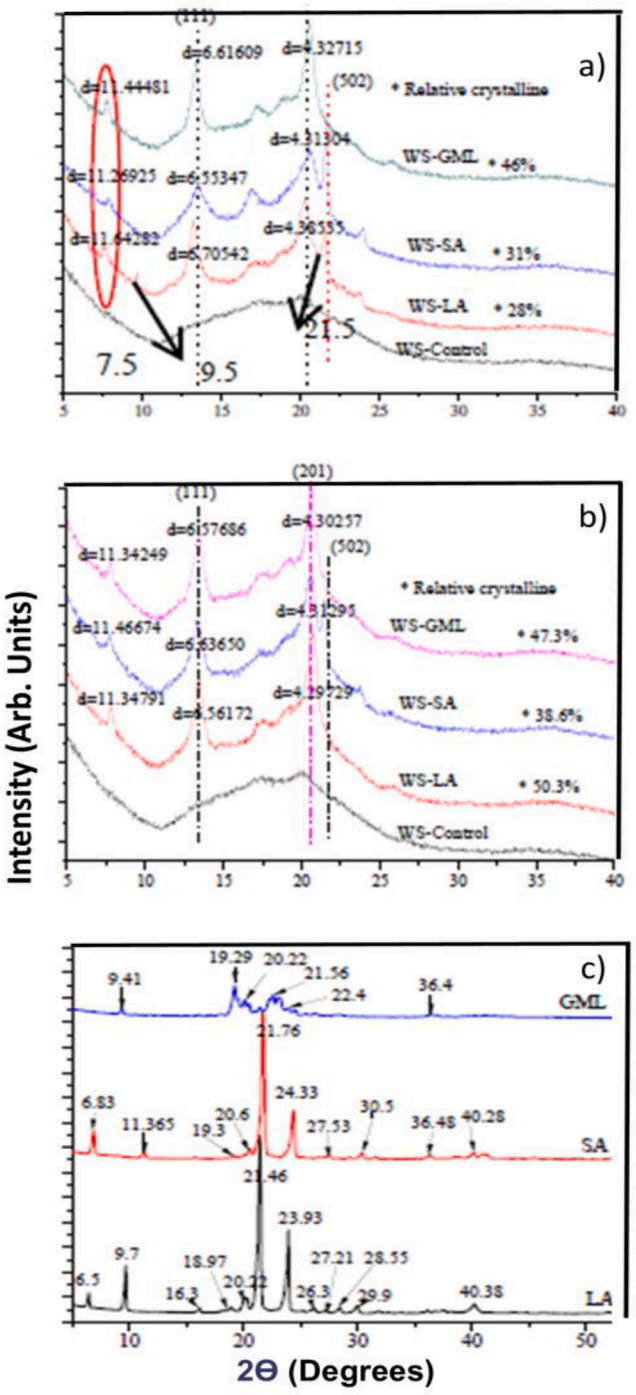

Fig. 4. X-ray diffraction patterns and relative crystalline of WS, WS-LA, WS-SA, and WS-GML samples. (a) water bath treatment, and (b) microwave treatment. (c) the X-ray diffraction patterns of LA, SA, and GML, respectively.

3.2. Scanning electron microscope (SEM)

The morphological characterizations of starch and fatty acid complexes formed under water bath and microwave heat treatment at 5000 × magnification are shown in Fig. 2 (a-h). Li et al., 2021 reported that the aggregation of starch-fatty acid complexes' crystal structures was similar to the semi-crystalline structure of polymers in parallel lamellar shapes. Fig. 2 (a & e) shows that large masses and rough surfaces were noticed in WS samples without lipid addition. Similar microstructures of starch-lipid complexes were perceived in a water bath and microwave-treated samples (Fig. 2 b-d & f-h). All prepared starch-lipid complexes samples showed dense, layered porous structure, except the water bath treated WS-SA sample. This phenomenon proves that WS-LA and WS-GML prepared by microwave (Fig. 1 b & d) cannot be stained using iodine solution. As the number of fatty acid carbon atoms increased, more parallel lamellae could be observed in both water bath, and microwave treated WS-GML samples than others. Additionally, samples treated with microwave heating showed more parallel lamellae than water bath treated ones. Combined with section 3.1, the parallel lamellae were positively correlated with complex content.

3.3. Fourier transform infrared spectroscopy analysis

As shown in Fig. 3 (a & b), the FTIR spectra of all samples were similar. In comparison with WS, new group characteristic peaks at 2850 cm^{-1} and 1710 cm^{-1}, assigned to asymmetric C—H stretching and C═O stretching vibration, were found in WS-LA and WS-SA samples, respectively. Moreover, an absorption band at 1735 cm^{-1} had appeared in the spectra when the GML was added to WS. In line with the results of *ISA*, obvious peaks at 2850 cm^{-1} and 1710 cm^{-1} might be attributed to the aggregation of free SA. This finding denotes no interplay between starch and lipids, and the binding mechanism could be ascribed to hydrophobic interaction. Further, compared with water bath treated WS-lipid samples, the infrared spectrum of 2850 cm^{-1} was absent in the microwave-treated samples because lipid was included in the amylose helix structure. This means that the corresponding groups were masked, and the less noticeable group meant that more lipid was wrapped by amylose helix, which is consistent with the changing trend of XRD results.

3.4. X-ray diffraction

X-ray diffraction was used to identify the crystalline structures of starch samples, formed by: the combined areas of crystalline and amorphous contributions, noise (background), and instrumental function (Rodriguez-Garcia et al., 2021; Londoño-Restrepo et al., 2019). To illustrate the diffraction peaks of starch-lipid complexes, the X-ray diffraction pattern of LA, SA, and GML are shown in Fig. 4c. Similar diffraction peaks were observed in LA and SA, different from the samples shown in Fig. 4 a and b, and Table 3. Two prominent intensity peaks at $2\theta = 13.4713^{\circ}$ and 20.5207°, corresponding to the (111) and (201) diffraction planes for the hexagonal structure and one small peak around 2θ of 7.8400° were displayed, respectively (Cervantes-Ramírez et al., 2020). Those characteristic peaks for the amylose–lipid complex were attributed to the crystallization of amylose–lipid complex with second derivative criteria 12.6278, 6.4622, and 4.3507 for 20.5207, 13.4713, and 7.8400°, respectively, which was similar to previous reports (Cervantes-Ramírez et al., 2020; Zabar, Lesmes, Katz, Shimoni & Bianco-Peled, 2010; Zhang, Huang, Luo & Fu, 2012; Zobel, 1988; Bhatnagar & Hanna, 1994a). The peaks observed for WS-GML and WS-LA were the tallest and clearest in the water bath and microwave heat treatment, respectively. These results illustrate that the optimal lipid chain lengths that form complexes with amylose might differ under different heating conditions. Notably, there were different assumptions on the optimum chain length that would favour the formation of starch-lipid complexes. Some evidence stated that lipids with a number of carbon atoms ≤ 10 are too short to induce amylose single helical structure formation, and lipid with 14 carbon atoms would be the best for inclusion complex formation. Others have declared that 16 or 18 carbon atoms are preferred (Putseys, Lamberts & Delcour, 2010; Karkalas et al., 1995; Krog & Jensen, 1970). As shown in Fig. 4b, the diffraction peaks of microwave-treated samples became higher and sharper than water bath treated ones. That is to say, the crystalline peaks of microwave heat-treated samples were sharper than those of water bath. This behaviour further elucidates that microwaves could promote the interplay between WS and lipid. During microwave treatment, the WS granules can swell and rupture within a short time under the effect of a fast heating rate, which in turn would trigger the release of amylose molecules. Further, the

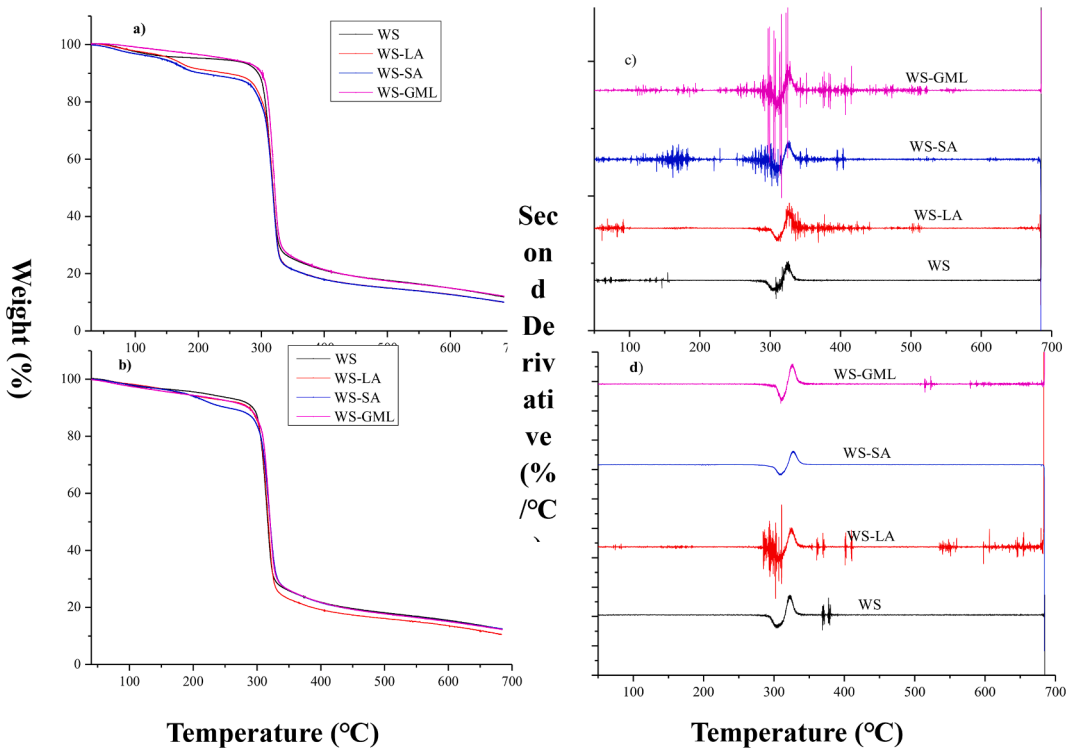

Fig. 5. Thermogravimetric and second derivative criteria curves of WS, WS-LA, WS-SA, and WS-GML samples. (a & c) water bath treatment, and (b & d) microwave treatment.

energy efficiency in the microwave is more intense than that of the water bath, which endows starch and lipid with higher energy density and increases the mobility of molecules, thereby promoting the formation of starch-lipid complexes. This finding was in line with the FTIR analysis results. In addition, diffraction peak at 2θ value = 9.5° and 21.8406°, corresponding to the crystalline pattern of LA and SA aggregates with a monoclinic crystalline structure, was observed in water bath treated WS-SA and WS-LA samples (Cervantes-Ramírez et al., 2020). In addition, there was a diffraction peak at 7.5°, which is different from the LA and SA aggregated peaks at around 6.5°. Therefore, it could be concluded that peaks that appeared at 7.5°, 13.4713°, and 20.5207° were the diffraction peaks with the formation of amylose–lipid complexes. It has to be noted that only WS-SA complexes treated with microwave heating showed small aggregates of SA diffraction peak. This result could be attributed to the fact that more ligand molecules interplay with amylose. Hence, fewer free lipids have remained in microwave-treated WS-lipid samples.

The relative crystallinity (RC) of WS-lipid samples treated with water bath and microwave heating, the ratio of crystalline domains, and amorphous regions (Gong et al., 2016) are shown in Fig. 4 (a & b). Compared with water bath treated samples, treatment with microwave results in a remarkable increase in RC (from 28% to 50.3% for WS-LA samples). Based on the FWHM of a characteristic peak, the calculation of the crystallinity percentage was carried out considering the complete XRD pattern (Londoño-Restrepo et al., 2019). The FHWM value of diffraction peak at 13.7° and 20.4° around 0.68, 0.62, and 0.83, 0.72 were lower in microwave treated WS-LA and WS-SA than water bath treated ones, corresponding to 0.69, 0.86, and 1.25, 1.33, respectively (Table 2). This finding demonstrates that the RC value is directly proportional to the diffraction peak intensity of starch and inversely proportional to the FHWM value.

3.5. Thermogravimetric analysis (TGA)

The analysis diagrams of TGA and second derivative criteria of the

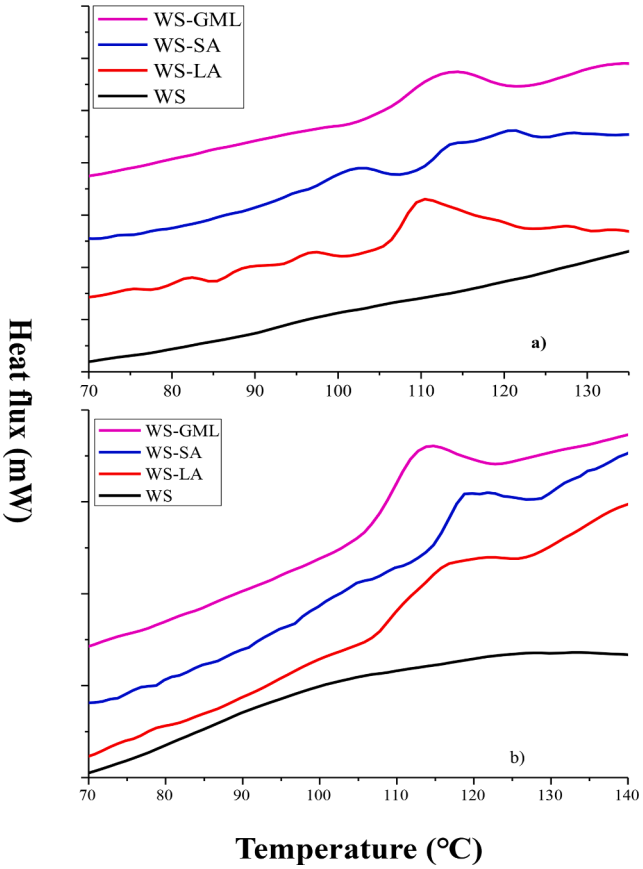

Fig. 6. Differential scanning calorimetry (DSC) curves of WS, WS-LA, WS-SA, and WS-GML samples. (a) water bath treatment, and (b) microwave treatment.

Table 1
The effect of heating on the formation of WS-lipid complexes.

Sample	T_o	T_p	T_c	ΔH
Water bath heating				
WS-LA	105.5 ± 2.8	108.9 ± 2.1	117.8 ± 2.9	6.8810 ± 0.37^a
WS-SA	93.6 ± 1.9	99.7 ± 1.2	106.0 ± 0.8	3.0470 ± 0.14^c
WS-GML	105.5 ± 3.0	112.4 ± 1.6	115.6 ± 1.1	4.3210 ± 0.11^b
Microwave heating				
WS-LA	104.1 ± 2.3	109.1 ± 1.5	119.4 ± 1.4	4.1580 ± 0.10^c
WS-SA	102.9 ± 1.1	111.3 ± 1.3	121.0 ± 1.7	4.8640 ± 0.27^b
WS-GML	102.8 ± 0.9	109.1 ± 2.0	117.6 ± 3.1	7.2860 ± 0.12^a

Onset temperature (T_o), peak temperatures (T_p), conclusion temperature (T_c), and enthalpy (ΔH). a-c: mean values in the same column with different superscripts are significantly different ($P < 0.05$).

water bath and microwaved WS-lipid complexes are shown in Fig. 5 (a-d). Experimental temperatures ranging from 30 to 700 ℃ and two main stages of weight loss were observed in all samples. The first stage related to the evaporation process of intramolecular water associates in crystals appeared near 150 ℃. The second thermal decomposition process of water bath treated WS-LA, WS-SA, and microwave treated WS-SA samples occurred between 170 and 300 ℃ that was 100 ℃ earlier than other samples. The reason could be attributed to hydrogen bonding between starch and ligand, which creates a compact structure that would enhance thermal stability to a certain extent. This result also proved that microwave treatment is more helpful in forming WS-lipid complexes than water bath treatment. In addition, the second derivative was used to identify each thermal transition.

3.6. Differential scanning calorimetry (DSC)

Thermograms of all WS-lipid complexes treated by microwave and water bath heating are revealed in Fig. 6 (a & b). The thermal parameters of endothermic peaks, including onset temperature (T_o), peak temperatures (T_p), conclusion temperature (T_c), and enthalpy (ΔH), are shown in Table 1. These values correspond to amylose–lipid complexes and content formed during water bath and microwave heat dissociation. All WS-lipid complex thermograms revealed T_p around 110 ℃, except for WS-SA complexes treated by water bath, which displayed melting point under 105 ℃ (Fig. 6b). The crystalline structure of starch-lipid complexes can be divided into types I and II at different temperatures. At a low reaction temperature, the formation of type I polymorphs was generally favoured through rapid nucleation coupled with an arrangement of helical segments randomly, with type I melting under 100 ℃.

On the other hand, type II polymorphs are usually obtained at a high reaction temperature by slow nucleation, with type II melting above 105 ℃ (Putseys et al., 2010; Putseys et al., 2009). Lower T_o value noticed in water bath treated WS-SA sample means forming disordered crystal structure (type I) than water bath treated WS-lipid complexes. In addition, compared with water bath treated WS-lipid complexes, the melting point increased from 99 to 111 ℃ during microwave heating. These findings could be attributed to the formation of type II WS-SA complexes during microwave heating. In addition, the high melting temperatures (T_p) of the complexes consist of crystals with ordered structures (Garcia, Pereira-Da-Silva, Taboga & Franco, 2016; Karkalas et al., 1995). This finding denotes that more ordered crystalline structures (type II) of WS-SA inclusion complexes are formed during microwaving than water bath heating. This finding is consistent with XRD results (microwave treated WS-SA displayed sharper and higher diffraction peaks). However, we observed no substantial differences between WS-LA and WS-GML treated by both methods. It was reported that only type II complexes could be displayed by XRD (Blazek & Gilbert, 2011), the finding which is at variance with our study. We may imply from the melting point that WS-SA prepared by water bath belongs to type I, whereas diffraction peaks for starch-lipid complexes were displayed in XRD.

Melting enthalpy (ΔH) used to measure the quantitative amount of starch-lipid inclusion complex is shown in Table 1 (Sandhu, Kaur, Singh & Lim, 2008). For samples prepared by water bath, the ΔH was inversely proportional to the chain length of lipid, denoting that short carbon chains would favour the formation of complexes (Zhang, Maladen & Hamaker, 2003). The ΔH of WS-SA and WS-GML prepared by water bath was lower than microwave treated ones. However, the ΔH of microwave

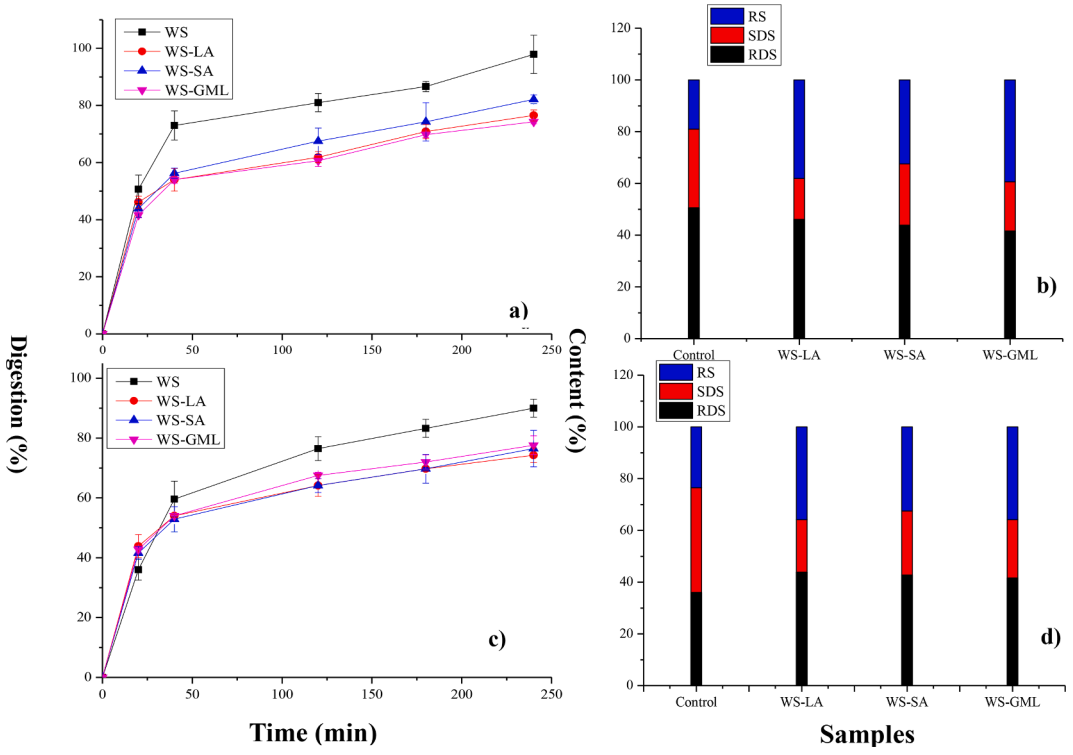

Fig. 7. *In vitro* digestibility curves of WS, WS-LA, WS-SA, and WS-GML samples. (a & b) water bath treatment, and (c & b) microwave treatment.

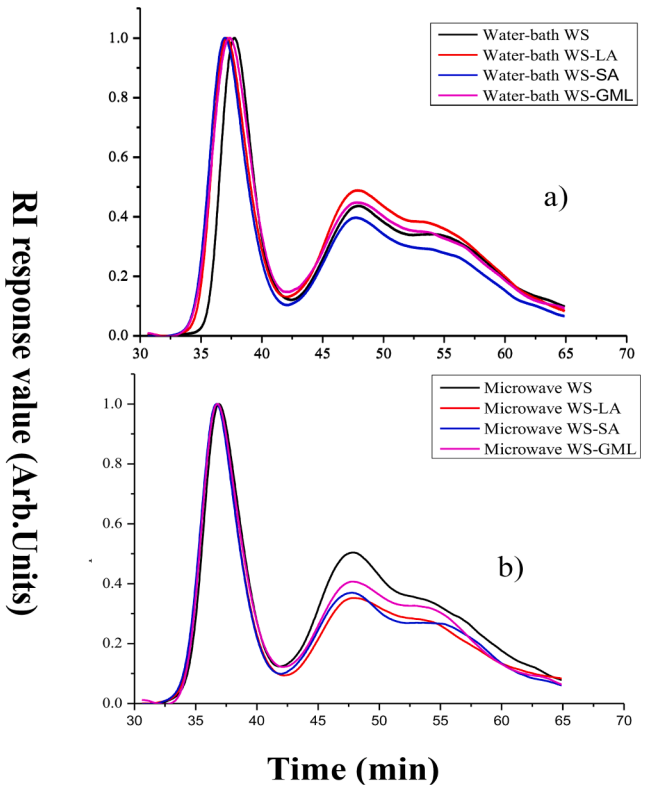

Fig. 8. Molecular size distribution curves of WS, WS-LA, WS-SA, and WS-GML samples. (a) water bath treatment, and (b) microwave treatment.

treated WS-LA sample (4.158 J/g) was lower than water bath (6.881 J/g). These results designate that more WS-SA and WS-GML and fewer WS-LA inclusion complexes were formed following microwave treatment, the finding which is at variance to XRD results. Therefore, from XRD and DSC results, it can be inferred that more type I complexes were formed during microwave treatment when LA was added, and more type II is formed with other lipids. In sum, microwave heating is a valuable and convenient way to form amylose–lipid complexes (RS_5).

3.7. *In vitro digestibility*

The hydrolysis plots for digestion of water bath and microwave heat treated WS samples with and without lipid incorporation are depicted in Fig. 7 (a & c). As shown, all samples exhibited similar hydrolysis plots with different lipid or treatments, whereas WS without lipid addition displayed a higher hydrolysis plot. WS and WS incorporated with lipids (LA, SA, and GML) for water bath treatment demonstrated a rapid increase in hydrolysis at the first 40 min. Then, a gradual increase to a plateau of 97.87 76.50, 82.13, and 74.25%, respectively. This phenomenon is in line with the results of XRD and DSC, documenting that short-chain fatty acids (inversely proportional to the hydrolysis rate) could form amylose–lipid complexes more easily. Similarly, for microwave treatment, WS and WS supplemented with lipids (LA, SA, and GML) showed a rapid increase in hydrolysis with increasing time at the early stage, which declines to 90, 74.5, 76.5, and 77.625% afterwards. It has to be noted that WS samples prepared by microwave had slightly lower hydrolysis than those prepared by a water bath. This finding indicates that more complexes were formed in microwave-treated samples. In other words, microwave promotes the interplay between amylose and ligand in the starch system.

To further investigate the resistance of WS-lipid complexes prepared by microwave to amylase hydrolysis, significant correlations between methods and RS, slowly digestible starch (SDS), and rapidly digestible starch (RDS) content of WS-lipid were monitored based on the above

Table 2
The full width at half maximum (FWHM) of XRD at 13° and 20°.

Samples	Water bath treatment		Microwave treatment	
	13°	20°	13°	20°
WS-LA	0.6969	0.8650	0.6838	0.6235
WS-SA	1.2587	1.3310	0.8344	0.7287
WS-GML	0.5924	0.7782	0.7404	0.7031

Table 3
Miller indexes, Bragg angles, and interplanar spacings for the hexagonal phase in the wheat starch-lipid complex.

Miller indexes	2θ(°)	*d*(Å) for Water bath treatment	*d*(Å) for Microwave treatment	Samples
(300)	7.8400°	11.1118	11.3425	WS-GML
		11.2693	11.4667	WS-SA
		11.6428	11.3479	WS-LA
(111)	13.4713°	6.6161	6.5769	WS-GML
		6.5535	6.6365	WS-SA
		6.7054	6.5617	WS-LA
(310)	20.5207°	4.3272	4.3026	WS-GML
		4.3130	4.3130	WS-SA
		4.3854	4.2973	WS-LA

results. Total starch hydrolyzed within 20 and 120 min is depicted in Fig. 7 (b & d). The addition of lipid significantly decreased the hydrolysis rate of inclusion complexes prepared by microwave or water bath heating. The reduction in the rate of hydrolysis might be accredited to the formation of amylose–lipid inclusion complexes between WS and lipids, making them not digested adequately by digestive enzymes than free amylose molecules because of their compact and ordered crystal structure. This outcome aligns with a prior study stating that pea starch-LA complex physicochemical performance was modified when exposed to maltogenic amylase and pullulanase (Liu, Gao, Zhang, Wu & Cui, 2020). As shown in Fig. 7, the RDS and RS contents of microwave-treated samples were lower than that of water bath treated ones, possibly because of increased production of type I complex in microwave treated samples, thereby increasing SDS content. In addition, the decline in hydrolysis rate was relevant to the structural level of the complex: the more type I crystalline complexes formed, the higher the SDS content after microwave heating. This result was in good agreement with the above conclusions. Further, it has been reported that SDS intake would result in a beneficial metabolic response to prevent and manage diabetes (Golay et al., 1992). Therefore, a starch-lipid complex prepared by this method would be helpful to establish a diabetes meal plan. Hence, microwave heating is one of the best ways to design starch with various functional components to create complexes that prevent elevated blood sugar levels.

3.8. *HPSEc*

The molecular size distribution of water bath, microwave treated WS, and WS-lipid samples are shown in Fig. 8 (a & b). Chromatogram profiles of all samples comprise readily distinguishable regions I, II, and III. The macromolecular size (region I) is principally from amylopectin, the medium-size molecule (region II) is primarily from intermediate materials of wheat starch, and the small molecular size (region III) is mainly from amylose. Compared with water bath treated WS, the area of region III decreased, and region I increased with lipid addition (Table 4). While for microwave heating, a considerable increase could be found in region I. An apparent decrease could be seen in regions II and III in WS-lipid samples than in samples without lipid. As compiled in Table 5, the microwave treated WS sample showed a higher Mw/Mn value than the

Table 4
The area ratio of different molecular sizes (region I, II, and III).

	Water bath treatment				Microwave treatment			
Region (%)	WS	WS-LA	WS-SA	WS-GML	WS	WS-LA	WS-SA	WS-GML
I	36.36	36.95	43.04	39.89	39.17	46.88	44.84	43.57
II	35.44	35.53	32.60	33.93	36.11	31.45	31.56	32.01
III	28.20	27.52	24.36	26.19	24.72	21.67	23.60	24.42

Table 5
The weight-average molecular weight (Mw), number-average molecular weight (Mn), and polydispersity index of all samples.

Samples	Mw (kDa)	Mn (kDa)	Polydispersity (Mw/Mn)
Water bath Control	48612.9	9659.7	5.033
Water bath LA	58299.8	9730.9	5.991
Water bath SA	65962.2	11,373	5.8
Water bath GML	54923.4	9300.7	5.905
Micro-control	51020.9	9151.6	5.575
Micro-LA	62709.9	11889.4	5.274
Micro-SA	60,155	11095.1	5.422
Micro-GML	58317.9	10668.7	5.466

water bath treated WS sample, indicating that the starch structure is entirely destroyed. Further, increased Mw values were observed in the water-bath and microwave treated samples with lipid, which illustrated the formation of complexes. However, the formation of starch-lipid complexes could not form a single size peak.

4. Conclusions

The crystalline structure, thermodynamic stability, molecular size, and *in vitro* digestion of WS-lipid samples prepared by microwave and conventional water bath treatments were tested to illustrate how microwave heating would affect the pasting properties of starches and interplay of amylose and lipid, structure, and starch digestibility. The formation of the WS-lipid complex was illustrated by *ISA* analysis. Further, the analysis of XRD suggested that the content of WS-lipid complexes formed in microwave treated samples was higher than that of water bath treated samples, implying that microwaves would promote the formation of starch-lipid complexes. LA and GML are the optimal carbon chain length for complex formation in the water bath and microwave heat treatment. Different effects on molecular size could be noticed in the microwave and water bath treated samples, verifying that these two heat treatments have varying degrees of destructive impacts on the structure of starch. Further, no new peak appeared with the formation of complexes, illustrating that the interplay between amylose and lipid does not influence its molecular size. In addition, the absorbance peaks that appeared at 2850 and 1750 cm^{-1} were eclipsed with the formation of starch-lipid complexes. More type I complex corresponds to slow digestible starch content in microwave treated samples based on thermodynamic and digestion procedures. In closing, microwave heating could be a suitable method for preparing starch-lipid complexes and benefit mass production.

CRediT authorship contribution statement

Xuemin Kang: Methodology, Investigation, Writing – original draft. **Siqiang Jia:** Investigation. **Wei Gao:** Investigation. **Bin Wang:** Investigation. **Xiaolei Zhang:** Investigation. **Yaoqi Tian:** Visualization. **Qingjie Sun:** Visualization. **Mohammed Atef:** Writing – review & editing. **Bo Cui:** Conceptualization, Resources, Supervision, Funding acquisition. **A.M. Abd El-Aty:** Formal analysis, Validation, Visualization, Writing – review & editing.

Declaration of Competing Interest

The authors declare that they have no known competing financial interests or personal relationships that could have appeared to influence the work reported in this paper.

Acknowledgements

The financial supports received from the National Key Research & Development Program in China (2019YFD1002704), the Key Research and Development Program of Shandong Province (2017YYSP024), Special Funds for Taishan Scholars Project, the Innovation Team of Jinan City (2018GXRC004), Shandong major projects of independent innovation (2019JZZY010722), the Science and Technology Demonstration Project of "Bohai Granary" of Shandong Province (2019BHLC002), Innovation Pilot Project of Integration of Science, Education and Shandong Province (2020KJC-ZD011), and Major agricultural application technology innovation projects of Shandong Province (SF1405303301) are acknowledged.

Authors' contribution

Xuemin Kang: Methodology, Investigation, Writing – original draft. Wei Gao: Investigation. Bin Wang: Investigation. Siqiang Jia & Xiaolei Zhang: Investigation. Yaoqi Tian & Qingjie Sun: Visualization. M. Atef: Writing-Review & Editing. Bo Cui: Conceptualization, Resources, Supervision, Funding acquisition. A. M. Abd El-Aty: Formal analysis, Validation, Visualization, Writing-Review & Editing.

References

Biliaderis, C. G., Page, C. M., Slade, L., & Sirett, R. R. (1985). Thermal-behavior of amylose-lipid complexes. *Carbohydrate Polymers, 5*(5), 367–389.
Blazek, J., & Gilbert, E. P. (2011). Application of small-angle X-ray and neutron scattering techniques to the characterisation of starch structure: A review. *Carbohydrate Polymers., 85*, 281–293.
Buddrick, O., Jones, O. A. H., Hughes, J. G., Kong, I., & Small, D. M. (2015). The effect of fermentation and addition of vegetable oil on resistant starch formation in wholegrain breads. *Food Chemistry, 180*, 181–185.
Casasnovas, J., & Anantheswaran, R. C. (2016). Dynamic measurement of starch granule swelling during microwave heating. *Carbohydrate Polymers, 151*, 1052–1057.
Cervantes-Ramírez, J. E., Cabrera-Ramirez, A. H., Morales-Sánchez, E., Rodriguez-García, M. E., Reyes-Vega, M. de L., Ramírez-Jiménez, A. K., Contreras-Jiménez, B. L., & Gaytán-Martínez, M. (2020). Amylose-lipid complex formation from extruded maize starch mixed with fatty acids. *Carbohydrate Polymers, 246*, 116555.
Cheng, W., Luo, Z., Li, L., & Fu, X. (2015). Preparation and characterization of debranched-starch/phosphatidylcholine inclusion complexes. *Journal of Agricultural and Food Chemistry, 63*(2), 634–641.
Eliasson, A. C., & Krog, N. (1985). Physical properties of amylose monoglyceride complexes. *Journal of Cereal Science, 3*(3), 239–248.
Englyst, H. N., & Cummings, J. H. (1985). Digestion of the polysaccharides of some cereal foods in the human small intestine. *American Journal of Clinical Nutrition, 42*(5), 778.
Evans, A., Mcnish, N., & Thompson, D. B. (2003). Polarization colors of lightly iodine-stained maize starches for amylose-extender and related genotypes in the W64A inbred line. *Starch-Stärke, 55*(6), 250–257.
Fan, D. M., Ma, S. Y., Wang, L. Y., Zhao, H. F., Zhao, J. X., Zhang, H., & Chen, W. (2013). ^{1}H NMR studies of starch-water interactions during microwave heating. *Carbohydrate Polymers, 97*, 406–412.
Fan, D. M., Ma, W. R., Wang, L. Y., Huang, J. L., Zhang, F. M., Zhao, J. X., … Chen, W. (2013). Determining the effects of microwave heating on the ordered structures of rice starch by NMR. *Carbohydrate Polymers, 92*(2), 1395–1401.
Fan, D. M., Wang, L. Y., Ma, S. Y., Ma, W. R., Liu, X. M., Huang, J. L., … Chen, W. (2013). Structural variation of rice starch in response to temperature during microwave heating before gelatinisation. *Carbohydrate Polymers, 92*(2), 1249–1255.

Fan, D. M., Wang, L. Y., Chen, W., Ma, S. Y., Ma, W. R., Liu, X. M., … Zhang, H. (2014). Effect of microwave on lamellar parameters of rice starch through small-angle X-ray scattering. *Food Hydrocolloids, 35*, 620–626.

Galloway, G. I., Biliaderis, C. G., & Stanley, D. W. (1989). Properties and structure of amylose-glycerol monostearate complexes formed in solution or on extrusion of wheat-flour. *Journal of Food Science, 54*, 950–957.

Garcia, M. C., Pereira-Da-Silva, M. A., Taboga, S., & Franco, C. M. L. (2016). Structural characterization of complexes prepared with glycerol monoestearate and maize starches with different amylose contents. *Carbohydrate Polymers, 148*, 371–379.

Gelders, G. G., Goesaert, H., & Delcour, J. A. (2005). Potato phosphorylase catalyzed synthesis of amylose-lipid complexes. *Biomacromolecules, 6*(5), 2622–2629.

Gelders, G. G., Vanderstukken, T. C., Goesaert, H., & Delcour, J. A. (2004). Amylose-lipid complexation: A new fractionation method. *Carbohydrate Polymers, 56*(4), 447–458.

Gong, B., Liu, W., Tan, H., Yu, D., Song, Z., & Lucia, L. A. (2016). Understanding shape and morphology of unusual tubular starch nanocrystals. *Carbohydrate Polymers, 151*, 666–675.

Golay, A., Koellreutter, B., Bloise, D., Assal, J. P., & Würsch, P. (1992). The effect of muesli or cornflakes at breakfast on carbohydrate metabolism in type 2 diabetic patients. *Diabetes Research and Clinical Practice, 15*(2), 135–141.

Kadokawa, J. I., Kaneko, Y., Nagase, S. I., Takahashi, T., & Tagaya, H. (2015). Vine-twining polymerization: Amylose twines around polyethers to form amylose-polyether inclusion complexes. *Chemistry, 8*(15), 3321–3326.

Kang, X. M., Yu, B., Zhang, H. Y., Sui, J., Guo, L., Abd El-Aty, A. M., & Cui, B. (2021). The formation and *in vitro* enzymatic digestibility of starch-lipid complexes in steamed bread free from and supplemented with different fatty acids: Effect on textural and retrogradation properties during storage. *International Journal of Biological Macromolecules, 166*, 1210–1219.

Karkalas, J., Ma, S., Morrison, W. R., & Pethrick, R. A. (1995). Some factors determining the thermal properties of amylose inclusion complexes with fatty acids. *Carbohydrate Research, 268*, 233–247.

Krog, N., & Jensen, B. N. (1970). Interaction of monoglycerides in different physical states with amylose and their anti-firming effects in bread. *Journal of Food Technology, 5*, 77–87.

Le-Bail, P., Houinsou-Houssou, B., Kosta, M., Pontoire, B., Gore, E., & Le-Bail, A. (2015). Molecular encapsulation of linoleic and linolenic acids by amylose using hydrothermal and high-pressure treatments. *Food Research International, 67*, 223–229.

Li, Q., Dong, Y. Y., Gao, Y., Du, S. K., Li, W. H., & Yu, X. Z. (2021). Functional properties and structural characteristics of starch-fatty acid complexes prepared at high temperature. *Journal of Agricultural and Food Chemistry*. https://doi.org/10.1021/acs.jafc.1c00110

Lin, L., Guo, D., Zhao, L., Zhang, X., Wang, J., Zhang, F., & Wei, C. (2016). Comparative structure of starches from high-amylose maize inbred lines and their hybrids. *Food Hydrocolloids, 52*, 19–28.

Liu, P. F., Gao, W., Zhang, X. L., Wu, Z. Z., & Cui, B. (2020). Physicochemical properties of pea starch-lauric acid complex modified by maltogenic amylase and pullulanase. *Carbohydrate Polymers, 242*, Article 116332.

Liu, P. F., Fang, Y. S., Zhang, X. L., Zou, F. X., & Cui, B. (2020). Effects of multienzyme treatment on the physicochemical properties of maize starch-lauric acid complex. *Food Hydrocolloids, 107*, Article 105941.

Londoño-Restrepo, S. M., Jeronimo-Cruz, R., Millán-Malo, B. M., Rivera-Muñoz, E. M., & Rodriguez-García, M. E. (2019). Effect of the nano crystal size on the X-ray diffraction patterns of biogenic hydroxyapatite from human, bovine, and porcine bones. *Scientific Reports, 9*(1), 5915.

Nimz, O., Gessler, K., Isabel, U., Sheldrick, G. M., & Saenger, W. (2004). Inclusion complexes of V-amylose with undecanoic acid and dodecanol at atomic resolution: X-ray structures with cycloamylose containing 26 D-glucoses (cyclohexaicosaose) as host. *Carbohydrate Research, 339*(8), 1427–1437.

Ozel, B., Dag, D., Kilercioglu, M., Sumnu, S. G., & Oztop, M. H. (2017). NMR relaxometry as a tool to understand the effect of microwave heating on starch-water interactions and gelatinization behavior. *LWT-Food Science and Technology, 83*, 10–17.

Putseys, J. A., Derde, L. J., Lamberts, L., Goesaert, H., & Delcour, J. A. (2009). Production of tailor made short chain amylose-lipid complexes using varying reaction conditions. *Carbohydrate Polymers, 78*(4), 854–861.

Putseys, J. A., Lamberts, L., & Delcour, J. A. (2010). Amylose-inclusion complexes: Formation, identity and physico-chemical properties. *Journal of Cereal Science, 51*(3), 238–247.

Rodriguez-Garcia, M. E., Hernandez-Landaverde, M. A., Delgado, J. M., Ramirez-Gutierrez, C. F., Ramirez-Cardona, M., Millan-Malo, B. M., & Londoño-Restrepo, S. M. (2021). Crystalline structures of the main components of starch. *Current Opinion in Food Science, 37*, 107–111.

Sandhu, K. S., Kaur, M., Singh, N., & Lim, S. T. (2008). A comparison of native and oxidized normal and waxy corn starches: Physicochemical, thermal, morphological and pasting properties. *LWT-Food Science & Technology, 41*, 1000–1010.

Siegfried, W. (2007). Book ReviewCyclodextrins and Their Complexes: Chemistry, Analytical Methods, Applications (Helena Dodziuk, Ed.). *Synthesis, 2007(14),* 2236-2236.

Soong, Y. Y., Goh, H. J., & Henry, C. J. K. (2013). The influence of saturated fatty acids on complex index and *in vitro* digestibility of rice starch. *International Journal of Food Sciences and Nutrition, 64*, 641–647.

Sullivan, W. R., Hughes, J. G., Cockman, R. W., & Small, D. M. (2018). The effects of temperature on the crystalline properties and resistant starch during storage of white bread. *Food Chemistry, 228*, 57–61.

Yuan, T., Yan, B. W., Fan, D. M., Zhang, N. N., Ma, S. Y., Wang, L. Y., … Zhang, H. (2020). Structural changes of starch subjected to microwave heating: A review from the perspective of dielectric properties. *Trends in Food Science & Technology, 99*, 593–607.

Zabar, S., Lesmes, U., Katz, I., Shimoni, E., & Bianco-Peled, H. (2010). Structural characteriztion of amylose-long chain fatty acid complexes produced via the acidification. *Food Hydrocolloids, 24*, 347–357.

Zhang, B., Huang, Q., Luo, F. X., & Fu, X. (2012). Structural characterizations and digestibility of debranched high-amylose maize starch complexed with lauric acid. *Food Hydrocolloids, 28*, 174–181.

Zhang, G., Maladen, M. D., & Hamaker, B. R. (2003). Detection of a novel three component complex consisting of starch, protein, and free fatty acids. *Journal of Agricultural and Food Chemistry, 51*, 2801–2805.

Zheng, B., Wang, H. W., Shang, W. T., Xie, F. W., Li, X. X., Chen, L., & Zhou, Z. K. (2018). Understanding the digestibility and nutritional functions of rice starch subjected to heat-moisture treatment. *Journal of Functional Foods, 45*, 165–172.

Zhou, Z. K., Robard, K., Helliwell, S., & Blanchard, C. (2007). Effect of the addition of fatty acids on rice starch properties. *Food Research International, 40*, 209–214.